Convective Heat Transfer Coefficients of Automatic Transmission Fluid Jets with Implications for Electric Machine Thermal Management

Preprint

Kevin Bennion and Gilberto Moreno
National Renewable Energy Laboratory

CONVECTIVE HEAT TRANSFER COEFFICIENTS OF AUTOMATIC TRANSMISSION FLUID JETS WITH IMPLICATIONS FOR ELECTRIC MACHINE THERMAL MANAGEMENT

Kevin Bennion
National Renewable Energy Laboratory
Golden, Colorado, USA

Gilberto Moreno
National Renewable Energy Laboratory
Golden, Colorado, USA

ABSTRACT

Thermal management for electric machines (motors/generators) is important as the automotive industry continues to transition to more electrically dominant vehicle propulsion systems. Cooling of the electric machine(s) in some electric vehicle traction drive applications is accomplished by impinging automatic transmission fluid (ATF) jets onto the machine's copper windings. In this study, we provide the results of experiments characterizing the thermal performance of ATF jets on surfaces representative of windings, using Ford's Mercon LV ATF. Experiments were carried out at various ATF temperatures and jet velocities to quantify the influence of these parameters on heat transfer coefficients. Fluid temperatures were varied from 50°C to 90°C to encompass potential operating temperatures within an automotive transaxle environment. The jet nozzle velocities were varied from 0.5 to 10 m/s. The experimental ATF heat transfer coefficient results provided in this report are a useful resource for understanding factors that influence the performance of ATF-based cooling systems for electric machines.

INTRODUCTION

Without the ability to remove heat, electric machines cannot operate without sacrificing performance, efficiency, and reliability. The ability to remove heat from the electric machine depends on the passive stack thermal resistances within the electric machine and the convective cooling performance of the selected cooling technology. The passive thermal design refers to the geometrical layout, material selection, and thermal interfaces that affect the heat spreading capabilities within the electric machine. The ability for heat to spread through the electric machine affects the thermal temperature gradients within the electric motor or generator. The convective cooling

technology is the cooling mechanism that ultimately removes the heat from the electric machine and transfers the heat to another location to reject the heat to the ambient environment. The technical challenge of electric machine thermal management is summarized by Hendershot and Miller as "[h]eat transfer is as important as electromagnetic and mechanical design. The analysis of heat transfer and fluid flow in electric machines is actually more complex, more nonlinear, and more difficult than the electromagnetic behavior." [1]. The performance benefit of convective heat transfer cooling designs are impacted by the passive stack thermal resistances within the electric machine. Prior work highlighted potential areas where thermal improvements to electric machines could impact performance [2]. Specifically, it was shown that for direct-cooled (e.g., ATF-cooled) motors, improving the convective cooling performance can significantly increase the total heat rejected.

Direct End-Winding Cooling

This work provides data on the convective heat transfer coefficients of automatic transmission fluid (ATF) jets impinging on surfaces representative of electric machine end windings. Figure 1 provides a cut cross section view illustrating general convective cooling approaches for automotive traction drive applications. One approach to cooling the electric machine includes a cooling water jacket incorporated into the housing that surrounds the stator. The water jacket is typically cooled with a mixture of water-ethylene glycol (WEG). Cooling of the electric traction drive machines in some vehicles is also accomplished by impinging ATF jets onto the copper windings [3,4]. Direct end-winding cooling with ATF is practical because ATF is a dielectric and, in some cases, the electric machines are housed within the vehicle's transmission

or transaxle where ATF is readily available. The thermal properties of ATF are inferior to those of WEG, which makes it a less effective coolant. However, the ability to use ATF to directly cool the rotor or end windings has significant advantages for removing heat. Directly cooling the end windings reduces the conduction path thermal resistance for heat generated within the windings.
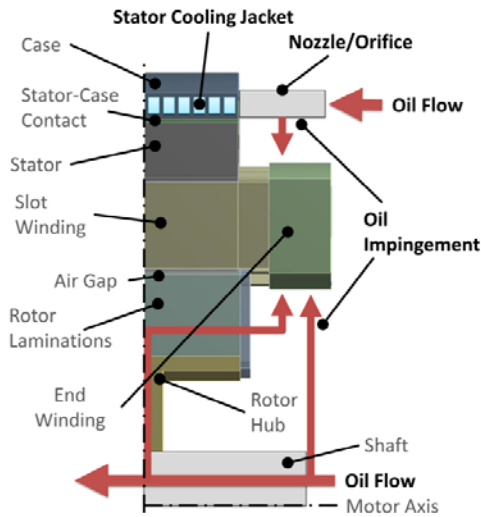
Figure 1. Cross section illustration of typical thermal management approaches incorporating a stator cooling jacket and oil cooling with ATF within the rotor and end windings.

Although direct cooling of the end winding with ATF is an approach for cooling electric machines in vehicle traction drive applications, currently there is minimal publicly available information regarding the jet impingement performance of ATF fluids. The flow of the ATF oil as it impinges onto the end winding is a complicated heat transfer and fluid dynamics problem. An understanding of the heat transfer of the ATF as it impinges onto the end windings is critical for electric machine designers in industry in order to maximize the performance of motors and generators while providing the required reliability and efficiency.

Oil Cooling Performance

While minimal, if any, information related to the thermal characteristics of ATF exists, there is literature available reporting thermal performance of viscous, high Prandtl number fluids (e.g., oils). Motor-scale studies have been conducted to evaluate oil cooling strategies for the electric machine. Davin et al. [5] experimentally evaluated various oil-cooling configurations for electric machines. Their experiments were conducted using a concentrated-winding stator and lubricating oil was used as the coolant. Their study was focused on evaluating methods to dispense the oil onto the stator using atomizing nozzles, an oil dripping manifold, and oil jet

configurations. Lim and Kim [6] evaluated different oil cooling configurations for an in-wheel electric machine using numerical and experimental analyses. Numerical analyses were conducted to optimize the oil spray distribution system. Experiments demonstrated that the optimized design allowed the electric machine to operate within its allowable operating temperatures.

In some cases, oil jets are employed to improve heat dissipation from combustion engines [7,8]. Easter et al. [7] conducted experiments to measure heat transfer coefficients of oil jets impinging on the underside of an engine piston. Their results indicate that heat transfer coefficients are insensitive to nozzle-to-surface distances but are influenced by oil temperatures. The results were then used to generate Nusselt number correlations. Liu et al. [8] also generated Nusselt number correlations for jets impinging on the underside of engine pistons. Their results demonstrated that oil-jet heat transfer coefficient increase with increasing oil temperatures. Images reveal that the oil jets atomize into a spray at the highest temperature (100°C). This atomizing effect is not observed at lower temperatures (30°C and 60°C).

Fundamental studies have also been conducted to characterize the heat transfer coefficients of impinging jets using oils as the working fluids. Metzger et al. [9] reported the heat transfer coefficients for synthetic-based lubricating oils and water free-jets discharged from a 58-cm-long tube. They developed average heat transfer coefficient correlations applicable to a wide range of Prandtl numbers (3 – 150). Additionally, it is reported that oil heat transfer coefficients decreased with increasing heater-diameter (D)-to-nozzle-orifice-diameter (d) ratios. Leland and Pais [10] also conducted experiments to measure the heat transfer coefficients of lubricating oil jets. They utilized an orifice-type nozzle and conducted tests in free-jet configurations. Over 700 data points were collected and used to develop average Nusselt number correlations. It is reported that varying the nozzle-to-heater distance (S) has minimal effect on heat transfer coefficients at the S/d ratios tested (S/d: 1.9 – 4.8). Sun et al. [11] characterized the radial heat transfer coefficients profiles for impinging transformer oil, R-113, and kerosene free-jets. Fluid Prandtl numbers varied from 7 to 262. They utilized a 35-mm-long and 1-mm-diameter tube as the nozzle. For all three fluids tested, the maximum heat transfer coefficients were obtained at the stagnation point, and heat transfer coefficients decreased with increasing radial distance (from the stagnation point). Moreover, the profiles of the normalized Nusselt numbers (stagnation point Nusselt number over the local Nusselt number) plotted versus the radial distance (r) were found to be nearly identical for all three fluids at $r/d < 3$. Ma, Zheng and Ko [12] measured the heat transfer coefficients for transformer oil free-jets using both plain-orifice and 35-mm-long tube nozzles. They provide local and average Nusselt number correlations for both nozzle types. They reported that the tube nozzle provides greater stagnation point heat transfer as compared with the orifice-type nozzle. Additionally, the importance of viscous heating effects with high Prandtl number fluids at higher Reynolds numbers was emphasized.

2

Ma, Zheng, et al. [13] conducted experiments using transformer oil in the submerged jet configuration. Slot jets of various nozzle dimensions were evaluated, and correlations were developed. As was the case with free jets, heat transfer coefficients were observed to achieve a maximum value at the stagnation point, then monotonically decrease with increasing lateral distance. Empirical correlations were used to predict the heat transfer coefficients of free jets in order to compare the performance of submerged jets to the performance of free jets. This comparison indicated that stagnation point heat transfer coefficients of the submerged jets were nearly identical to those provided by free jets. More information on the performance of submerged and free jets using transformer oil and ethylene glycol as the fluids was reported by Ma, Sun, et al. [14]

In this study, we provide the results of experiments characterizing the thermal performance of ATF free-jets. Tests were conducted to evaluate the effects of ATF temperature and nozzle jet velocity on heat transfer coefficients. Plain target surfaces were tested, and the results were compared with correlation-predicted results. In addition, target surfaces with features simulating machine wire bundles of various wire gauges were tested and results were compared.

EXPERIMENTAL APPARATUS AND PROCEDURES

Fluid Test Loop

The test loop was designed and fabricated to characterize the forced convection thermal performance of ATF. A schematic of the experimental test loop is provided in Figure 2. The loop can be configured to conduct jet impingement or channel flow tests and can accommodate a variety of test articles (e.g., small test heaters or larger electric machines). Fluid flow rates of up to 20 liters per minute (LPM) and fluid temperatures of up to 110°C can be produced by the system.
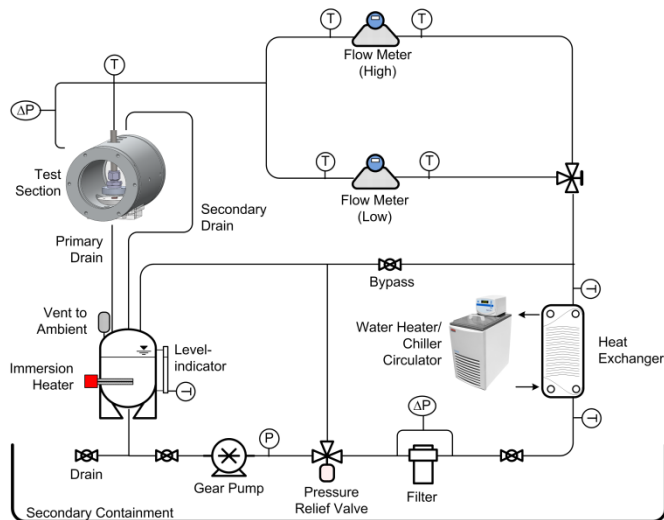
Figure 2. Test flow loop schematic.

Approximately 15 liters of Mercon LV ATF are contained within the loop. Mercon LV was evaluated in this study because

of its use in hybrid electric vehicles. Ford Motor Company provided thermal properties of the fluid. The fluid is circulated through the loop via a variable-frequency-drive-controlled gear pump. System fluid temperatures are controlled and held constant using a heater/chiller bath circulator and flat-plate heat exchanger system as well as an immersion heater located within the reservoir tank.

Instrumentation includes equipment for flow, temperature, and pressure measurements. Two Coriolis mass flow meters measure fluid-flow rates. The low-flow-rate flow meter has a range of $0 - 2$ LPM and provides accurate measurements at lower flow rates. The high-flow-rate flow meter has a range of $2 - 20$ LPM and allows for accurate measurements at higher flow rates. Temperature (K-type thermocouples) and pressure sensors are located throughout the loop as shown in Figure 2.

Impingement Test Section and Targets

The ATF jet impingement experiments were conducted within the test section shown in Figure 3. Fluid entered the test section through a tube at the top of the chamber. Fluid then flowed through a nozzle plate to generate an impinging jet onto the test sample. The nozzle was an orifice-type nozzle with a 2-mm orifice diameter (d). Drain ports at the front and back of the vessel allowed the fluid to drain through gravity and create a free-jet condition (i.e., non-flooded). A thermocouple located just upstream of the test section measured the fluid inlet temperature. A differential pressure transducer measured the pressure drop across the nozzle. Viewports on the front and back of the test section enabled visualization of the experiments as shown in Figure 3.
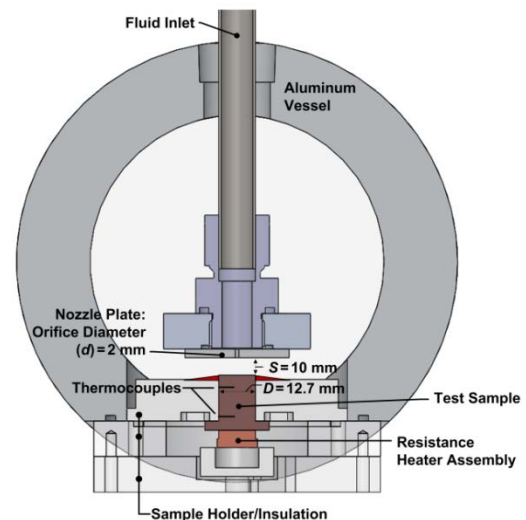
Figure 3. Schematic of the test section showing the nozzle and test sample.

Figure 4 plots the pressure drop across the nozzle versus the jet velocity at the three fluid temperatures tested. This nozzle was utilized for all experiments presented in this study. The trend seen in Figure 4 illustrates that the pressure drop

increases as the velocity/flow rate increases. This result aligns with accepted theories in fundamental fluid dynamics. The pressure drop is also seen to decrease for increasing inlet temperatures at the same nozzle velocity. This effect is associated with lower ATF viscosities at higher temperatures, which results in the observed decrease in pressure drop.
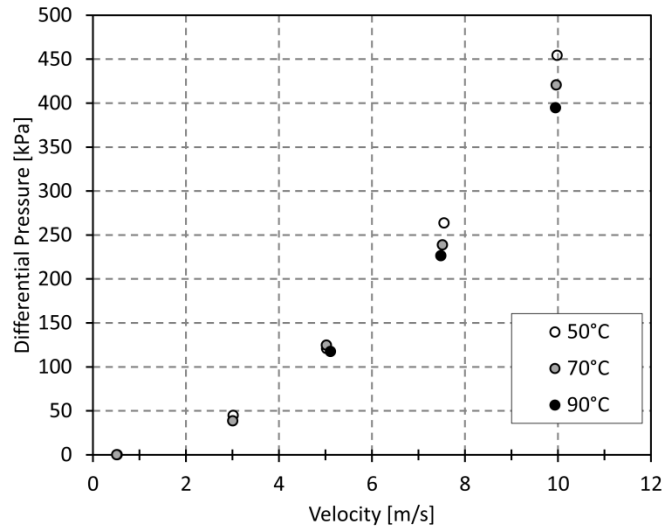
Figure 4. Differential pressure drop across the nozzle plotted versus the jet velocity.

The test target samples, which were fabricated from oxygen-free copper, had an impingement or cooled surface diameter (D) of 12.7 mm. The copper test samples were inserted into Teflon disks ("sample holder/insulation" part in Figure 3) for support and thermal insulation. A combination of high-temperature silicone sealant and epoxy was applied around the test samples and between the samples and Teflon to prevent fluid leaks. Two calibrated K-type thermocouples were embedded within the sample to measure heat fluxes and to calculate surface/wall temperature. The sample was heated using a computer-controlled power supply that powered a resistance heater assembly attached to the lower side of the sample. Thermal interface material (grease) applied between the resistance heater assembly and the test sample reduced the contact resistance between the resistance heater assembly and the test sample. Figure 5 shows the assembled test target in the experimental setup, and Figure 6 shows the setup with an impinging AFT fluid jet.
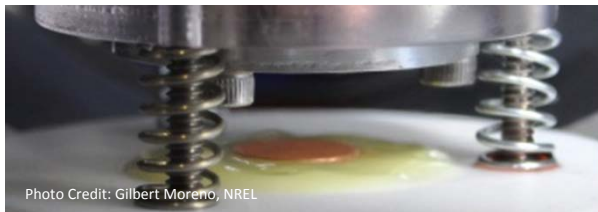
Figure 5. Picture of test section showing target.
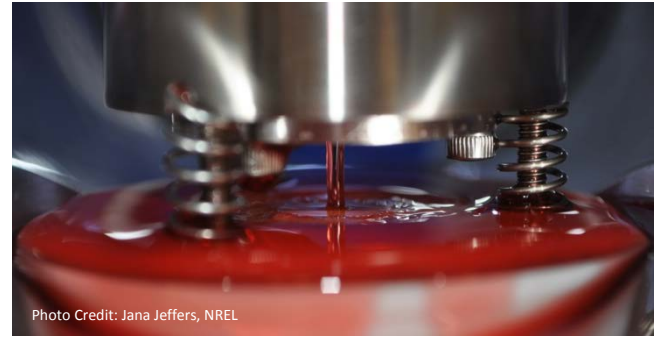
Figure 6. Picture of test section showing ATF jet impinging on target.

The thermal performance of four test samples with different surface features were evaluated under jet impingement (free-jet) cooling conditions. The baseline sample was sandpaper-polished (600 grit) to create a smooth impingement surface. The other three samples were fabricated (via wire electrical discharge machining) with surface features that were intended to simulate wire bundles found in electric machines. The features on these samples consisted of a series of parallel circular ridges running straight across the impingement surface (Figure 7 and Figure 8). The radius of these ridges corresponds to the radius of the American wire gauge (AWG) (e.g., 18 AWG, 22 AWG, or 26 AWG) plus the thickness of the wire insulation based on Polyurethane-180 heavy build insulation from MWS Wire Industries. The relevant dimensions of these test samples along with impingement surface area measurements are provided in Table 1.
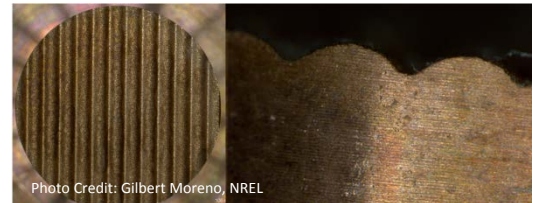
Figure 7. 18 AWG surface target: Top view (left), side view (right).

Table 1. Test sample feature dimensions and surface area measurements

	Baseline	18 AWG	22 AWG	26 AWG
Radius, mm (wire and insulation)	N/A	0.547	0.351	0.226
Total wetted surface area, mm^2	126.7	148.2	143.3	139.2

4
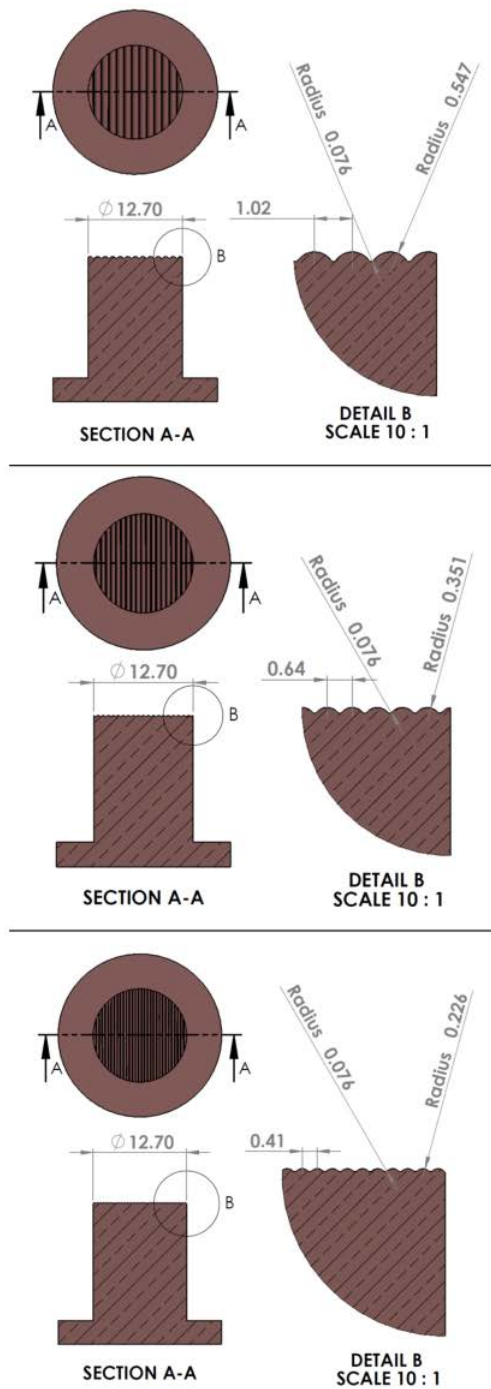
Figure 8. Computer-aided design models of the 18 AWG (top), 22 AWG (middle), and 26 AWG (bottom) samples. Dimensions shown are in millimeters. The top 12.7-mm-diameter surface was the jet impingement surface.

Experimental Procedure

The procedure for initiating experimental tests was consistently applied for each of the tested surfaces. The nozzle and test sample assembly were aligned vertically and the nozzle-to-impingement-surface distance (S) was set to 10 mm (S/d = 5). The test sample and nozzle assembly were then installed within the test section. The gear pump was activated, and the fluid was circulated through the loop. The bath circulator and the immersion heater were then turned on to achieve the desired test section fluid inlet temperature. Once the system reached the set point temperature, the pump speed was adjusted and the bypass valve was throttled to achieve the desired nozzle flow rate. Upon achieving the desired fluid conditions, the experiments were initiated.

A LabVIEW program controlled and monitored experiments via a data acquisition system and direct current power supply. For these experiments, the power supply powered the resistance heater that heated the test sample. Power was adjusted to achieve a test sample impingement surface temperature of approximately 110°C. Once temperature equilibrium was reached, the program recorded temperature, pressure, and flow rate data and calculated the heat transfer coefficient values. For every case, the heat transfer coefficients ($\bar{h}$) were defined according to Equation 1.

$$\bar{h} = \frac{Q}{A_p(T_w - T_l)} \qquad (1)$$

Q is the heat dissipated through the top 12.7-mm-diameter surface, and T_w is the sample's average impingement surface temperature. Both values (Q and T_w) were calculated via the two thermocouples embedded within the test sample, assuming one-dimensional, steady-state heat transfer. Due to the highly conductive properties of the oxygen-free copper samples, the calculated surface temperature (T_w) is taken to be an average of the surface temperatures. In other words, T_w is the average temperature of the stagnation and wall-jet regions on the test sample. For the baseline sample, T_w is the average impingement surface temperature. For the other samples, T_w is calculated at a plane of constant cross-sectional area just below the surface protrusions/features. A_p is the surface area of the 12.7-mm-diameter impingement area (the increased surface area from the features in the 18 AWG, 22 AWG, and 26 AWG samples is not included), and T_l is the temperature of the liquid jet, as measured by the thermocouple probe immediately upstream of the nozzle. System parameters relevant to this study are summarized in Table 2. Every test condition was repeated a minimum of three times.

Table 2. Test Sample Feature Dimensions and Surface Area Measurements

D (mm)	d (mm)	S (mm)	S/d	D/d
12.7	2.06	10	5	6.2

5

RESULTS AND DISCUSSION

Experiments were conducted to characterize the thermal performance of Mercon LV ATF impinging free jets. The effect of fluid jet velocity and temperature on heat transfer coefficients was measured. Jet velocities of approximately 0.5 m/s, 2.8 m/s, 5 m/s, 7.5 m/s, and 10 m/s and fluid temperatures of 50°C, 70°C, and 90°C were studied. A significant amount of fluid heat was lost to the ambient environment at the highest fluid temperature tested. This prevented us from conducting experiments at lower fluid velocities with a fluid temperature of 90°C. Therefore, 90°C fluid temperature experiments were only conducted at velocities equal to or greater than 5 m/s. The higher jet velocities examined in this project are not currently used within automotive ATF machine cooling applications. These elevated velocities were evaluated here to characterize the thermal performance of ATF fluids over a wide jet velocity range.

Figure 9 displays the average heat transfer coefficient results for the baseline sample at inlet fluid temperatures of 50°C, 70°C, and 90°C. The heat transfer coefficient results provided are an average of all test runs completed. The error bars represent 95% uncertainty incorporating random and systematic uncertainties. As expected, the heat transfer coefficients increased with increasing impinging jet velocity. Varying the inlet temperature had minimal influence on heat transfer coefficients for the flat target surface. The results are compared against available correlations in the literature [9,10,12] over the valid ranges of the correlations. The baseline experimental results are within the range of the correlations, considering the uncertainty in the measurements, correlations, and fluid properties. Within the experimental measurement uncertainties, it is not possible to distinguish a clear impact of inlet fluid temperature on the measured average convective heat transfer coefficient.
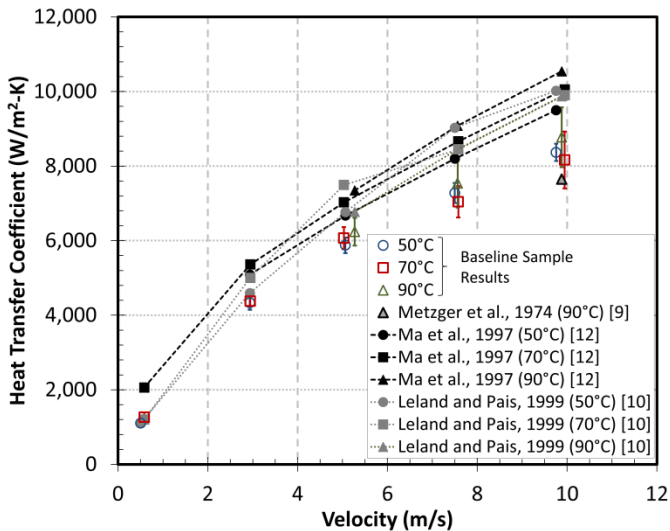
Figure 9. Baseline sample heat transfer coefficient results compared to literature correlations.

Figures 10, 11, and 12 compare data from all samples tested at inlet temperatures of 50°C, 70°C, and 90°C, respectively. All the heat transfer coefficient values are averaged values computed from multiple test runs for each sample. At the lowest jet velocity tested (0.5 m/s), all four samples provided about the same performance (Figure 10 and Figure 11).
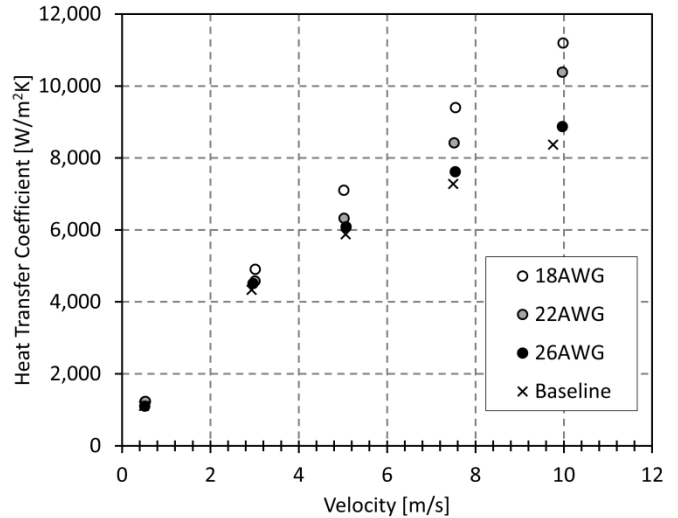
Figure 10. Heat transfer coefficients of all target surfaces at 50°C inlet temperature.
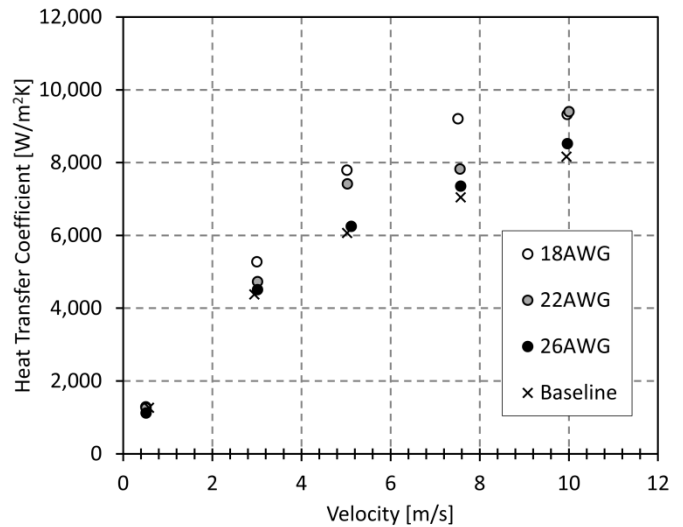
Figure 11. Heat transfer coefficients of all target surfaces at 70°C inlet temperature.

This suggests that the wire bundle features of the 18 AWG, 22 AWG, and 26 AWG samples had minimal effect on performance at this low jet velocity (i.e., a jet velocity consistent with automotive ATF electric machine cooling applications). Variations in the performance of the samples are more apparent at higher jet velocities. At more elevated jet

6

velocities, the 18 AWG and 22 AWG test samples did provide some heat transfer coefficient enhancement as compared to the baseline sample. In all cases, the 26 AWG sample and the baseline sample produced almost identical results, indicating that the surface features on this sample had minimal effect on performance with ATF.
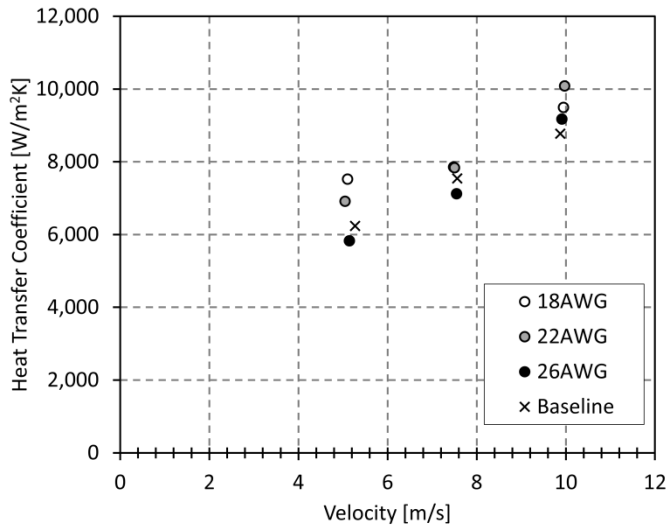
Figure 12. Heat transfer coefficients of all target surfaces at 90°C inlet temperature.

For the 50°C temperature case (Figure 10), the heat transfer coefficient results for the various samples are in line with the surface area measurements provided in Table 1—the greater the surface area, the higher the heat transfer coefficients. At 50°C, the 18 AWG sample, which has the highest surface area, outperformed all samples. At lower jet velocities, the test samples with the wire features perform similarly to the baseline flat surface.

The performance trends at higher fluid temperatures are less clear. At 70°C and 90°C (Figures 11 and 12), fluid splatter was observed for the 18 AWG, 22 AWG, and 26 AWG samples at higher jet velocities. This phenomenon is associated with fluid being deflected off the surface by the samples' round, protruding features. This deflection reduced the amount of fluid supplied to the outer sections of the samples, leading to reduced convective heat transfer performance. This effect was a random, uncontrolled event leading to variation in the results and was more pronounced with the 18 AWG and 22 AWG samples. Evidence of this splattering effect is indicated by a plateau in the heat transfer coefficient curves at the higher jet velocities as seen in Figure 11. The effect is less clear at 90°C in Figure 12, but the 18 AWG sample shows the largest effects due to fluid splattering. Figure 13 shows images of the ATF jet impingement with and without the fluid splatter.

Photo Credit: Jana Jeffers, NREL

Photo Credit: Jana Jeffers, NREL
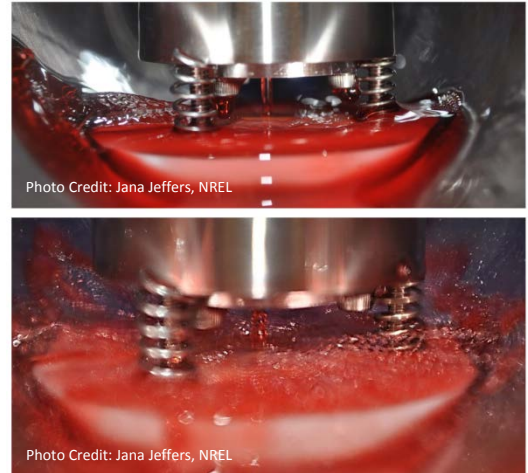
Figure 13. ATF flowing over surface (top), ATF deflecting off surface (bottom).

Figure 14 represents only data from the 18 AWG sample and focuses on the trends in the heat transfer coefficient with increasing jet velocity and inlet temperature. For the 50°C inlet temperature, the heat transfer coefficient increases almost linearly with nozzle velocity. At this temperature, the surface splattering described above did not occur.
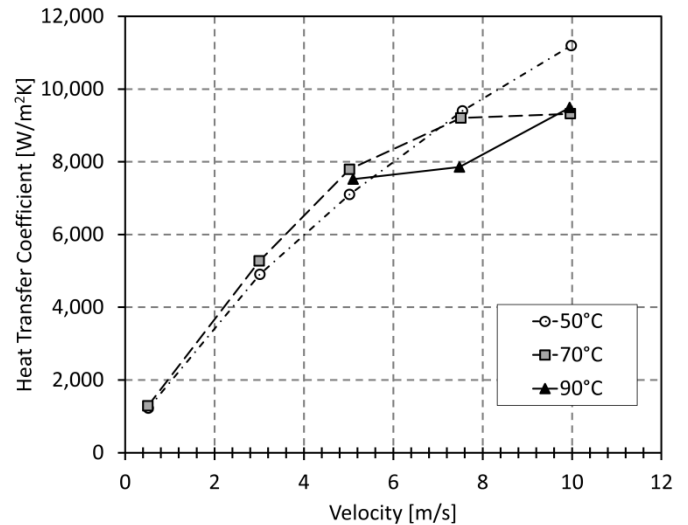
Figure 14. Heat transfer coefficients of 18 AWG sample for all inlet temperatures.

At a 70°C inlet temperature and at approximately 7.5 m/s, the fluid impinged on the center of the sample surface and moved outward over the entire surface. Conversely, at 10 m/s, some of the fluid deflected off the surface immediately after impingement, and this effect is manifested as a plateau in the 70°C heat transfer coefficient curve at the higher velocities. In the 90°C data, fluid splatter was observed to occur at lower velocities. Because the fluid splatter was more prevalent at higher temperatures, we speculate that the lower ATF

viscosities at higher temperatures are more conducive to this splattering effect. It is assumed that the fluid viscosity influences the splattering effect.

CONCLUSIONS

This paper provides data for free-jet impingement convective heat transfer coefficients of Mercon LV ATF applicable to end-winding cooling of electric machines. The direct impingement of ATF on end windings has been shown to be an effective approach for cooling electric machines used in electric vehicle traction drive applications. Prior sensitivity analysis [2] has shown that the convective cooling performance on the electric machine's end winding can have a significant impact on the ability to remove heat from an electric machine or generator. The resulting improvement in heat removal directly influences the power rating of the electric machine and the reliability of temperature sensitive components such as insulation materials and magnets. Currently, limited information is available in the open literature quantifying the convective heat transfer coefficients of ATF jets impinging on end-winding surfaces of electric machines. This work was initiated to quantify average ATF jet impingement heat transfer coefficients on surfaces representative of end windings.

A test fixture was designed to measure average heat transfer coefficients of ATF jets in the free-jet configuration. The test fixture is capable of fluid flow rates up to 20 LPM (3.33e-4 m^3/s) and fluid temperatures up to 110°C. In the work described in this paper, the ATF temperatures were varied from 50°C to 90°C, and jet nozzle velocities were varied from 0.5 m/s to 10 m/s. Two calibrated thermocouples provided measurements for heat flux and the target surface/wall temperature, which enabled calculating heat transfer coefficients. In addition to the calculated heat transfer coefficient, pressure measurements were also recorded to measure the pressure drop of the ATF jet through the orifice nozzle.

The results of this study highlight the influence of surface topology, fluid temperature, and jet velocity on convective heat transfer coefficients. For the baseline target surface, increasing the jet velocity increased heat transfer, but fluid temperature had negligible effect on heat transfer coefficients. At low jet velocities the wire-bundle features on test samples (18 AWG, 22 AWG, and 26 AWG) had minimal effect on heat transfer coefficients at the lowest jet velocity tested (0.5 m/s). At this low velocity, all three test samples yielded nearly identical results that were similar to the results for the baseline sample. At higher jet velocities, the 18 AWG and 22 AWG samples, for the most part, provided heat transfer values greater than those of the baseline sample. The performance of the 26 AWG sample mirrored that of the baseline sample at all temperatures and jet velocities. Fluid splattering resulting in ATF deflecting off of the impingement surface was observed to occur on the 18 AWG, 22 AWG, and 26 AWG samples at higher jet velocities (≥7.5 m/s). This effect reduced the fluid available for heat removal potentially contributing to bulk warming of the fluid and thus reduced heat transfer coefficients. This phenomenon was more pronounced with the two samples that had the larger surface features (i.e., 18 AWG and 22 AWG). The pressure drop across the nozzle was found to decrease with increasing fluid temperatures. This effect is associated with lower ATF viscosities at higher temperatures. Lower pressure drop implies lower parasitic power losses. The results presented here not only provide data for ATF jet impingement on surfaces representative of end-winding wire bundle, but the work also identified limitations for increasing convective heat transfer through increased jet velocity.

Future work is planned to further evaluate the forced convection heat transfer of ATF impingement on end windings. This current work focused on measurements of average heat transfer coefficients directly aligned with the fluid jet. In actual applications, the heat transfer coefficient would not be uniform. The variation in heat transfer coefficient is due partly to the variation in the local heat transfer coefficient away from the stagnation point of the jet impinging on the surface. On a larger scale, the heat transfer coefficient also varies because not all of the end winding is directly impinged upon by the jet. Some regions on the end winding are limited to the available ATF flowing over the surface away from the jet impingement area. Future work will focus on these two areas to measure the local heat transfer coefficient around the stagnation zone, and measure larger scale heat transfer variation on in-situ tests on electric machine end windings.

ACKNOWLEDGMENTS

NOMENCLATURE

A_p	Heated surface area (projected)
ATF	Automatic transmission fluid
D	Heater diameter
d	Nozzle orifice diameter
h	Heat transfer coefficient
Q	Heat
r	Radial distance
S	Nozzle-to-heater distance
T_l	Liquid temperature
T_w	Wall temperature

REFERENCES

[1] Hendershot, J. R., and Miller, T. J. E., 1994, Design of Brushless Permanent-Magnet Motors, Magna Physics Pub., Oxford, UK

[2] Bennion, K., and Cousineau, J., 2012, "Sensitivity Analysis of Traction Drive Motor Cooling," IEEE Transportation Electrification Conference and Expo (ITEC), pp. 1–6.

[3] Brooke, A. L., 2011, Chevrolet Volt: Development Story of the Pioneering Electrified Vehicle, SAE International.

[4] Burress, T., Coomer, C., Campbell, S., Wereszczak, A., Cunningham, J., Marlino, L., Seiber, L., and Lin, H.-T., 2009, "Evaluation of the 2008 Lexus LS 600H Hybrid Synergy Drive System." ORNL/TM-2008/185, Oak Ridge National Laboratory, Oak Ridge, TN.

[5] Davin, T., Pellé, J., Harmand, S., and Yu, R., 2015, "Experimental Study of Oil Cooling Systems for Electric Motors," Appl. Therm. Eng., **75**, pp. 1–13.

[6] Lim, D. H., and Kim, S. C., 2014, "Thermal Performance of Oil Spray Cooling System for in-Wheel Motor in Electric Vehicles," Appl. Therm. Eng., **63**(2), pp. 577–587.

[7] Easter, J., Jarrett, C., Pespisa, C., Liu, Y. C., Alkidas, A. C., Guessous, L., and Sangeorzan, B. P., 2014, "An Area-Average Correlation for Oil-Jet Cooling of Automotive Pistons," J. Heat Transf., **136**(12), pp. 124501–124501.

[8] Liu, Y., Guessous, L., Sangeorzan, B., and Alkidas, A., 2014, "Laboratory Experiments on Oil-Jet Cooling of Internal Combustion Engine Pistons: Area-Average Correlation of Oil-Jet Impingement Heat Transfer," J. Energy Eng., p. C4014003.

[9] Metzger, D. E., Cummings, K. N., and Ruby, W. A., 1974, "Effects of Prandtl Number on Heat Transfer Characteristics of Impinging Liquid Jets.," Int. Heat Transf. Conf 5th Proc, Tokyo, Japan, pp. 20–24.

[10] Leland, J. E., and Pais, M. R., 1999, "Free Jet Impingement Heat Transfer of a High Prandtl Number Fluid Under Conditions of Highly Varying Properties," J. Heat Transf., **121**(3), pp. 592–597.

[11] Sun, H., Ma, C. F., and Chen, Y. C., 1998, "Prandtl Number Dependence of Impingement Heat Transfer with Circular Free-Surface Liquid Jets," Int. J. Heat Mass Transf., **41**(10), pp. 1360–1363.

[12] Ma, C. F., Zheng, Q., and Ko, S. Y., 1997, "Local Heat Transfer and Recovery Factor with Impinging Free-surface Circular Jets of Transformer Oil," Int. J. Heat Mass Transf., **40**(18), pp. 4295–4308.

[13] Ma, C. F., Zheng, Q., Lee, S. C., and Gomi, T., 1997, "Impingement Heat Transfer and Recovery Effect with Submerged Jets of Large Prandtl Number Liquid—I. Unconfined Circular Jets," Int. J. Heat Mass Transf., **40**(6), pp. 1481–1490.

[14] Ma, C. F., Sun, H., Auracher, H., and Gomi, T., 1990, "Local Convective Heat Transfer from Vertical Heated Surfaces to Impinging Circular Jets of Large Prandtl Number Liquid," Proceedings of the Ninth International Heat Transfer Conference, Jerusalem, Israel, pp. 441–446.